Available online at www.sciencedirect.com
SCIENCE DIRECT®
Journal of Solid State Chemistry 177 (2004) 1535–1541
JOURNAL OF SOLID STATE CHEMISTRY
http://elsevier.com/locate/jssc

Preparation and characterization of $NiO_{(core)}/Fe_2O_{3(shell)}$ composite particles

L. Xiang,* Y.P. Yin, and Y. Jin

Department of Chemical Engineering, Tsinghua University, Beijing 100084, China

Received 3 September 2003; received in revised form 24 November 2003; accepted 8 December 2003

Abstract

A novel hydrothermal coating process has been developed to deposit amorphous $Ni(OH)_2 \cdot H_2O$ over octahedral α-Fe_2O_3 particles by treating aqueous dispersion of the preformed cores in $Ni(NO_3)_2/CH_3COONa$ solution. $NiO_{(core)}/Fe_2O_{3(shell)}$ composite particles were prepared by air sintering of the $Ni(OH)_2 \cdot H_2O_{(shell)}/Fe_2O_{3(core)}$ particles at 200–500°C for 1–6 h. The changes of morphology, structure and weight of the hydrothermal and sintering products were studied by means of TEM, XRD, XPS, TG and IR analyzers. The nucleation and growth model was suggested for the non-isothermal decomposition of $Ni(OH)_2 \cdot H_2O$ coatings and the kinetic equation was derived from the non-linear regression of the TG data. The activation in the thermal-decomposition process is $73.8\,kJ\,mol^{-1}$ and the pre-exponential factor is $1.95 \times 10^4\,s^{-1}$.

Keywords: Hydrothermal coating; Thermo-decomposition; Nickel hydroxide; Nickel oxide; Iron oxide

1. Introduction

Over recent years, there has been growing interest in the chemical synthesis of advanced ceramic materials. One area that is receiving considerable attention is the use of coated particles. The deposition of a functional layer on the surface of individual inorganic particles constitutes an important topic in powder technology, because the surface properties of the generated core-shell particles can be altered to meet the required specifications in various fields such as catalysis, ceramics, pigment, corrosion, etc. [1]. Therefore, the special structure of the core-shell composite particles made it quite important in theoretical studies and in applied research.

Up to now a large number of studies have been done for the synthesis of the coated particles [2–13]. Compared with other routes for the preparation of the coated powders such as precipitation [8,12], urea decomposition [10,11], electro-less plating [9], sol–gel method [2–5] seems to be used most commonly owing to its ability to prepare coatings with a wide variety of chemical compositions. However, most of the reported sol–gel techniques are still limited in laboratory scale due to some un-resolving deficits such as the strict condition for the formation of coatings, the complexity or the high cost involved in the sol–gel coating procedure. Therefore, some hydrothermal coating researches have emerged to overcome the above shortcomings. The literatures published in recent time show that hydrothermal method is a promising method to fabricate the coated particles owing to its high reaction speed, the controllable compositions of coatings, the simplicity and moderate conditions for the formation of coatings [6–7,13].

In this paper, an advanced hydrothermal technology has been developed to synthesize core-shell composite particles-forming $Ni(OH)_2 \cdot H_2O$ film on the surface of Fe_2O_3 particles. The thermo-decomposition behavior of the hydrothermal products, including the variation of the morphology and structure of the sintering products with heating temperature and time, were investigated. The non-linear regression methods were used to identify the kinetic mechanism involved in the non-isothermal decomposition of the $Ni(OH)_2 \cdot H_2O$ coatings.

*Corresponding author. Fax: +86-1-062-772-051.
E-mail address: xianglan@flotu.org (L. Xiang).

0022-4596/$ - see front matter © 2003 Elsevier Inc. All rights reserved.
doi:10.1016/j.jssc.2003.12.004

2. Experimental

2.1. Sample preparation

A commercial sample of α-Fe_2O_3 was used in this work. The core-shell composite particles were synthesized by treating the Fe_2O_3 particles in aqueous solution containing CH_3COONa and $Ni(NO_3)_2$ at elevated temperature. For this purpose 15.00 g of α-Fe_2O_3 particles was first ultrasonically suspended in 150 mL of an aqueous solution containing 0.5 mol/L CH_3COONa and 0.5 mol/L $Ni(NO_3)_2$; the dispersion was then transferred to a stainless steel autoclave with an inner volume of 250 cm^3. After sealing, the suspension was magnetically stirred (450 min^{-1}) and the autoclave was heated (5°C/min) gradually to 200°C and kept for 4.0 h. After hydrothermal treatment, the autoclave was cooled down to room temperature naturally, the resulting suspensions were filtrated and the solids were washed several times with distilled water. Finally, the coated powders were dried at 105°C for 12 h and stored in a desiccator.

The sintering experiments were carried out in an electric furnace (Model SX2-10-13, Shanghai Kangtai Co., Ltd., China). The composite particles formed via hydrothermal coating methods were heated from ambient to 200–500°C at a heating rate of 20°C min^{-1} and then maintained the later temperature in isothermal conditions for 1–6 h. After sintering, the samples were left to cool naturally in the furnace.

2.2. Analyses

The morphology of the samples was examined with a scanning electron microscope (SEM, Model JSM-6301, JEOL, Japan) and transmission electron microscope (TEM, Model JEM-200CX, JEOL, Japan). Powder X-ray diffraction (XRD) patterns of the samples were obtained with a D/Max-RB diffractometer using nickel-filtered Cu$K\alpha$ radiation. X-ray photoelectron spectroscope (XPS, Model PHI-5300, PHI, American) was used to confirm the existence of Ni on the surface of the coated particles and to identify the Ni-bearing phase. Infrared (IR) spectra were obtained using a Fourier transform infrared (FTIR) spectrometer (Model Nicolet 560, Nico, American).

Thermo-gravimetric analyzer (TGA, Model 2050, Beijing Optical Products Co., Ltd., China) was used to identify the thermal behavior of the hydrothermal product. The sample was heated under the static air atmosphere from ambient to 1000°C at a heating rate of 20°C min^{-1}. The particle was 7 ± 0.1 mg and the reference substance was alumina.

The weight of the Fe_2O_3 particles before and after hydrothermal coating treatment was measured by means of a digital electric balance (Model MP5028, Shanghai Jinke Electric Balance Company, China) with an accuracy of ± 0.01 g. The Ni content in the hydrothermal products was analyzed by dissolving an accurately weighted amount of the coated sample in 2 mol/L chloride acid and then analyzing of the resulting solution with an atomic absorption spectrophotometer (Model 3510, Agilent Technologies Shanghai, China) in an acetylene flame, the analysis accuracy is $\pm 2.0\%$.

3. Results and discussion

3.1. Hydrothermal formation and characterization of $Ni(OH)_2 \cdot H_2O_{(core)}/Fe_2O_{3(shell)}$ composite particles

Fig. 1 shows a TEM photomicrographs of the Fe_2O_3 particles before (a) and after (b) hydrothermal treatment The α-Fe_2O_3 particles (Fig. 1a) were nearly octahedral in shape, having a diameter of about 0.2–0.3 μm. Fig. 1b confirmed the existence of the film on the surface of the coated α-Fe_2O_3 particles. The comparison of the corresponding selected-area electron diffraction pattern analyses (Fig. 2) of the above samples indicated that the layer was mainly consisted of amorphous materials. Chemical analyses show that the weight percent of the deposit in the composite particles is 10.3% and the Ni

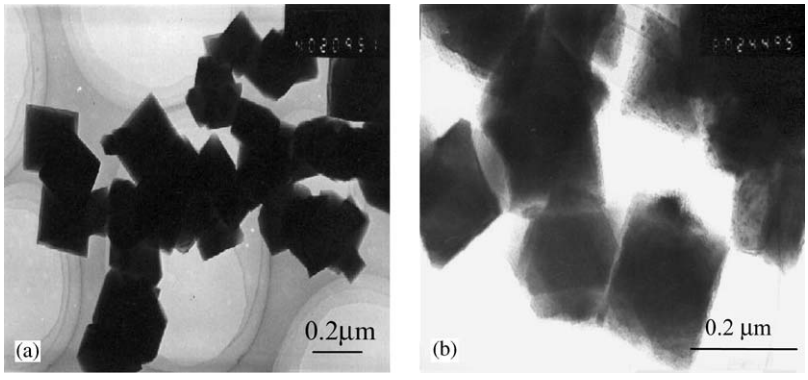

Fig. 1. Morphology of Fe_2O_3 particles before (a) and after (b) hydrothermal treatment.

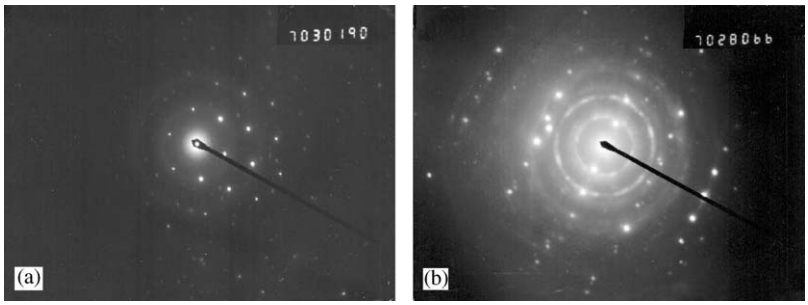

Fig. 2. Electron diffraction patterns of the α-Fe_2O_3 particles before (a) and after (b) hydrothermal treatment.

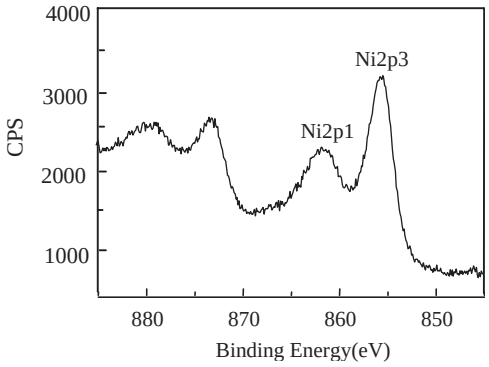

Fig. 3. XPS spectrum of Ni for the coated α-Fe_2O_3 powder.

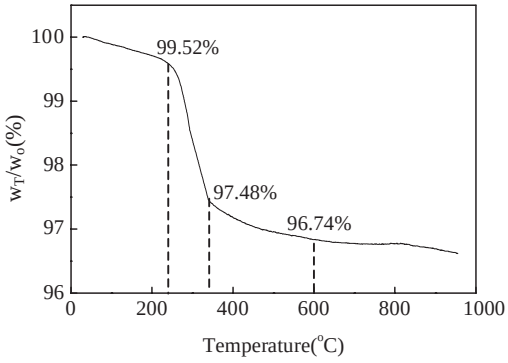

Fig. 4. TG curve of the $Ni(OH)_2 \cdot H_2O/Fe_2O_3$ composite particles.

contents in the deposit was 49.6 wt%. Fig. 3 shows the XPS spectra of Ni in the coated particles. The binding energy of Ni (Ni2p3, 855.56 eV) in the deposits is almost the same as that of $Ni(OH)_2$ (Ni2p3 855.60 eV), indicating that the film may be mainly composed of $Ni(OH)_2$.

CH_3COO^- is a weak electrolyte which tends to be hydrolyzed to CH_3COOH and OH^- in aqueous solution: $CH_3COO^- + H_2O \rightarrow CH_3COOH + OH^-$. The increase of temperature is favorable for the hydrolysis of CH_3COO^- or the formation of OH^- [14,15]. Therefore, it was suggested that the $Ni(OH)_2$ coatings may be formed via the hydrolysis of CH_3COO^- ions followed by the interaction of OH^- and Ni^{2+} ions. The consumption of OH^- and the accumulation of CH_3COOH might lead to the decrease of the solution pH. The experimental results indicated that the solution pH before and after hydrothermal coating treatment were 5.6 and 4.5, respectively. The decrease of solution pH with reaction time seems to confirm the above hypothesis.

The TG curve of the hydrothermal coating particles is shown in Fig. 4. The composite particles underwent a three-stage decomposition process. The induction stage was in the temperature range of 25–240°C with a weight loss of 0.48% due to the evaporation of the absorbed water; the acceleratory stage was in the temperature range of 230–335°C in which the weight loss increased quickly from 0.48% to 2.52%; the deceleratory period occurred at temperatures above 335°C due to the gradual consumption of the reactant. The total weight loss was about 3.26% at 600°C, which is quite close to the theoretical weight loss (3.35%) for the complete conversion of $Ni(OH)_2 \cdot H_2O_{(shell)}/Fe_2O_{3(core)}$ to $NiO_{(shell)}/Fe_2O_{3(core)}$ when the weight percent of the deposit in the composite particles is 10.3%.

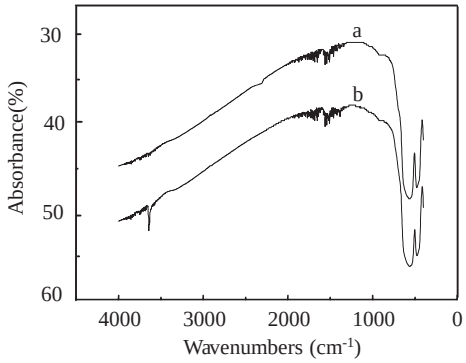

Fig. 5. FTIR spectra of α-Fe_2O_3 particles before (a) and after (b) hydrothermal treatment.

FTIR spectra of the Fe_2O_3 particles before and after hydrothermal treatment are listed in Fig. 5. Both of the samples were pre-heated at 240°C in air for 2 h before FTIR detection to avoid the influence of the absorbed water. Compared with the raw material, the hydrothermal product occurs an obvious absorption peak in

the range of 3500–3700 cm^{-1}, which may be attributed to the existence of O–H bond in $Ni(OH)_2 \cdot H_2O$.

3.2. Thermal-decomposition of the hydrothermal coating product

A series of sintering experiments were performed to investigate the influence of heating temperature and time on the morphology and structure of the sintering products, using the $Ni(OH)_2 \cdot H_2O_{(core)}/Fe_2O_{3(shell)}$ composite particles formed under hydrothermal condition. The typical morphology of the sintering product is shown in Fig. 6. Smooth film with a thickness of about 0.01 μm was formed on the surface of Fe_2O_3 particles after sintering of the hydrothermal coating particles at 500°C for 4 h. The variation of the XRD patterns of the sintering products with temperature and heating time are shown in Figs. 7 and 8, respectively. The amorphous $Ni(OH)_2$ coatings were gradually converted to films composed of NiO nano-crystals after sintering. The comparison of the data in Figs. 7 and 8 with the standard XRD database (ICSD database) indicates that the crystal structure of Fe_2O_3 belongs to hexagonal system with a rhomb-centered lattice ($a = 5.035$ Å, $c = 13.74$ Å) while the NiO crystals belong to cubic system with a face-centered lattice ($a = 4.176$ Å). The crystallinity of the NiO crystals improved with the increase of temperature or the prolongation of the sintering time. The variation of the NiO crystal sizes with the sintering temperature and heating time, estimated from the (200) crystal surface (corresponding to 2θ angle of 43.3°) by Scherrer formula ($d = 0.9\lambda/B(\cos\theta)$), were summarized in Tables 1 and 2, respectively. The sizes of NiO nano-crystals increased gradually (9.8–14.3 nm) with the increase of temperature from 200°C to 500°C or the increase of the heating time from 1 to 6 h.

The variation of the loss of the sintering product with the heating time at 400°C is shown in Fig. 9. Most of the $Ni(OH)_2 \cdot H_2O$ coatings were converted to NiO particles during the initial 0.5 h, leading to an obvious weight loss of about 3.20%; with further increase of the heating time from 0.5 to 4 h, less than 0.16% of the weight loss was observed.

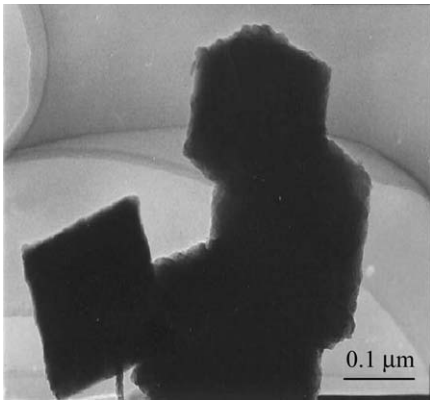

Fig. 6. Morphology of the sintering product. Temperature (°C): 500; time: 4 h.

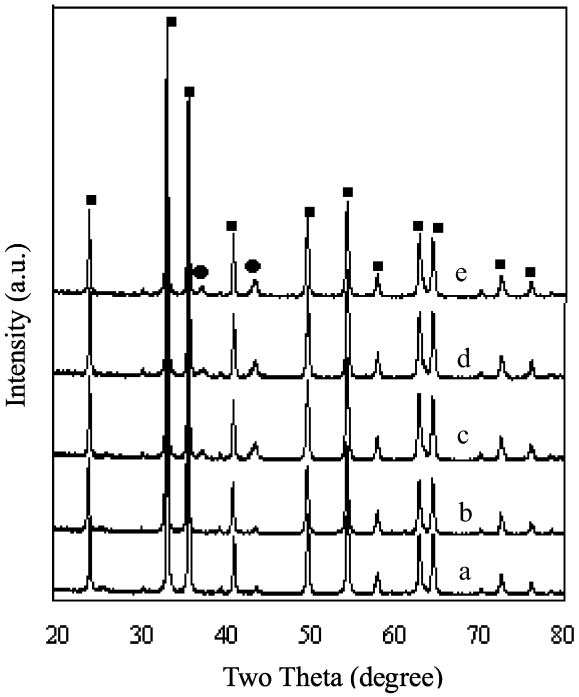

Fig. 7. XRD patterns of the sintering products formed at different temperatures. Temperature (°C): (a) raw material, (b) 200, (c) 300, (d) 400, (e) 500; time: 2 h. ■: α-Fe_2O_3, ●: NiO.

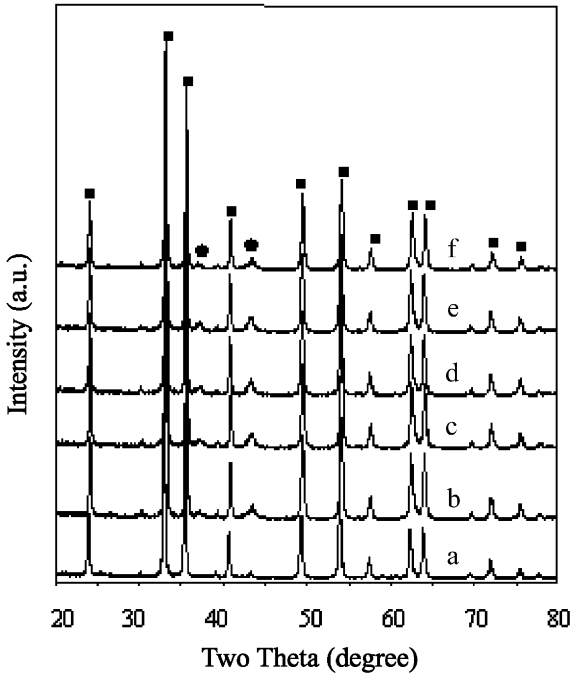

Fig. 8. XRD spectra of the sintering products formed at different time. Time (h): (a) raw material, (b) 0, (c) 1.0, (d) 2.0, (e) 4.0, (f) 6.0; temperature: 400°C. ■: α-Fe_2O_3, ●: NiO.

Table 1
Variation of the size of NiO crystallites with temperature

Temperature (°C)	200	300	400	500
Size of NiO crystallites (nm)	9.8	10.3	12.4	13.7

Time: 4 h.

Table 2
Variation of the sizes of NiO crystallites with heating time

Sintering time (h)	1	2	4	6
Size of NiO crystallite (nm)	10.9	12.4	13.4	14.1

Temperature: 400°C.

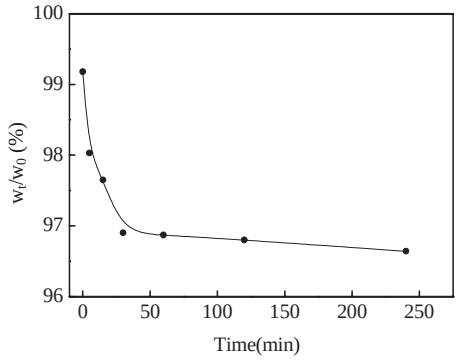

Fig. 9. Variation of the weight loss of the sintering product with the heating time. Temperature: 400°C.

3.3. Theory of non-isothermal thermogravimetry

The non-isothermal thermogravimetry (TG) with linear temperature increase is a method frequently used to characterize materials from the thermal behavior standpoint [16–20]. In addition, it enables determination of apparent kinetic parameters. The calculation methods are either based on a single TG curve or require several TG curves measured at various heating rates. The single curve methods are based on a regression of the fundamental kinetic equation. They are relatively satisfactory for simple processes.

Kinetic calculations from the thermo-gravimetric data usually proceed from the basic kinetic equation

$$\frac{d\alpha}{dt} = k(T)f(\alpha), \tag{1}$$

where α represents the transformation degree at time t, $f(\alpha)$ the conversion function dependent on mechanism of the reaction, and $k(T)$ the rate constant as a function of the absolute temperature T.

The forms of the conversion functions $f(\alpha)$ are dependent on the assumed reaction kinetic mechanisms which have been classified into three groups: the diffusion, the chemical reaction, and the nucleation models. The general $f(\alpha)$ form for the most common mechanism used in kinetics of solid-state decomposition is as follows [18]:

$$f(\alpha) = \alpha^m(1-\alpha)^n[-\ln(1-\alpha)]^p, \tag{2}$$

where m, n and p are kinetic parameters connected with the mechanism. The possible $f(\alpha)$ expressions and the corresponding kinetic mechanisms are detailed in Table 3.

Table 3
Algebraic expression of $f(\alpha)$ for the kinetic models of thermo-decomposition

Model number	$f(\alpha)$	Kinetic mechanism
1	α^m	$m = -1$, one dimensional diffusion $0 < m < 1$, power law
2	$(1-\alpha)^n$	$n = 1$, nucleation and growth $n = 1/2$, 2/3, interface reaction $n = 1.5$, 2, chemical reaction
3	$[-\ln(1-\alpha)]^p$	Two dimensional diffusion
4	$\alpha^m(1-\alpha)^n$	Self-catalytic reaction
5	$(1-\alpha)^n[-\ln(1-\alpha)]^p$	Nucleation and growth

3.4. Kinetic model of the non-isothermal decomposition

For the non-isothermal process with a constant heating rate:

$$\frac{dT}{dt} = \beta, \tag{3}$$

where β is the heating rate in the TG experiment ($0.33°C\,s^{-1}$).

Then the kinetic equation for the non-isothermal decomposition of the $Ni(OH)_2 \cdot H_2O$ coatings is as follows:

$$\frac{d\alpha}{dT} = \frac{A}{\beta}\exp\left(-\frac{E}{RT}\right)f(\alpha) \tag{4}$$

with α defined as

$$\alpha = \frac{w_{Ni,0} - w_{Ni,t}}{w_{Ni,0} - w_{Ni,e}}, \tag{5}$$

where $w_{Ni,0}$, w_{Ni} and $w_{Ni,e}$ are the weights of the $Ni(OH)_2 \cdot H_2O$ coatings at heating time 0 (before sintering), t and end of sintering, respectively.

The blank TG experiment confirmed that the weight of Fe_2O_3 particles remained constant in the temperature range of 200–600°C.

Then

$$\alpha = \frac{w_{N_i,0} - w_{N_i,t}}{w_{N_i,0} - w_{N_i,e}} = \frac{w_0 - w_t}{w_0 - w_e} = \frac{1 - w_t/w_0}{1 - w_e/w_0} \tag{6}$$

and

$$\frac{d\alpha}{dT} = -\frac{1}{1 - w_e/w_0}\frac{d(w_t/w_0)}{dT}, \tag{7}$$

where $w_{Fe,0}$, $w_{Fe,t}$, $w_{Fe,e}$ are the weight of Fe_2O_3 at heating time 0, t and end of sintering, respectively; w_0, w_t and w_e are the weight of the composite particles at time 0, t and end, respectively.

The values of $d(w_t/w_0)/dT$, w_e/w_0 and α_i at different temperatures (T_i) can be determined from the TG data in Fig. 4, then $(d\alpha/dT)_i$ can be calculated using Eq. (7). The calculated results are listed in Table 4.

3.5. Direct non-linear regression

Combining Eqs. (2) and (4) to give

$$\frac{d\alpha}{dT} = \frac{A}{\beta}\exp\left(-\frac{E}{RT}\right)\alpha^m(1-\alpha)^n[-\ln(1-\alpha)]^p. \quad (8)$$

Searching for these parameters is a typical non-linear regression problem. The kinetic parameters (m, n, p, E, and A) calculated from Eq. (8) and the TG curve in Fig. 4 are compared and optimized.

Table 4
The values of α_i and $(d\alpha/dT)_I$ at different temperatures

T_i (K)	α_i	$(d\alpha/dT)_i$
481.5	0	0.00064
483.5	0.00093	0.00066
493.7	0.00794	0.00089
503.2	0.01800	0.00117
513.4	0.0320	0.00155
523.6	0.0498	0.00237
533.8	0.0797	0.00412
543.3	0.1265	0.00631
548.7	0.1675	0.00752
553.5	0.2050	0.00877
558.2	0.2472	0.0103
563.6	0.3021	0.0128
568.4	0.3667	0.0155
573.8	0.4611	0.0184
578.5	0.5602	0.0197
583.3	0.6670	0.0193
588.7	0.7814	0.0165
593.4	0.8568	0.0128
598.2	0.9014	0.00888
603.6	0.9264	0.00533
613.7	0.9544	0.00242
623.8	0.9729	0.00174
633.2	0.9878	0.00140
643.2	0.9980	0.00121

There are a number of algorithms (optimization methods) for setting parameter values. To evaluate the set parameters, the residual sum of squares of deviations of experimental and calculated regression function values (RSS) is commonly used [15–18]. It is defined for Eq. (8) by the following relation:

$$\mathrm{RSS} = \sum_{i=1}^{k}\left\{\left(\frac{d\alpha}{dT}\right)_i - \frac{A}{\beta}e^{-E/RT}\alpha_i^m(1-\alpha_i)^n[-\ln(1-\alpha_i)]^p\right\}^2. \quad (9)$$

Table 5 shows the regression results of the experimental data with different $f(\alpha)$ models in Table 1. Model 1 was not considered despite its minimum RSS value since the value of the simulated activation energy is negative which is impossible in practice. The simulation curves for models 2–5 are shown in Fig. 10. Among these models, model 5 shows the least RSS value and the best fitness between the theoretical and the experimental data. Therefore, the conversion function of the thermodecomposition of the coatings can be expressed with the following equation according to the RSS minimum criterion:

$$\frac{d\alpha}{dT} = 1.95\times10^4\exp\left(-\frac{73.8}{RT}\right)(1-\alpha)^{0.97}[-\ln(1-\alpha)]^{0.35}. \quad (10)$$

It is concluded that the relevant thermal decomposition of the coating probably belongs to the nucleation

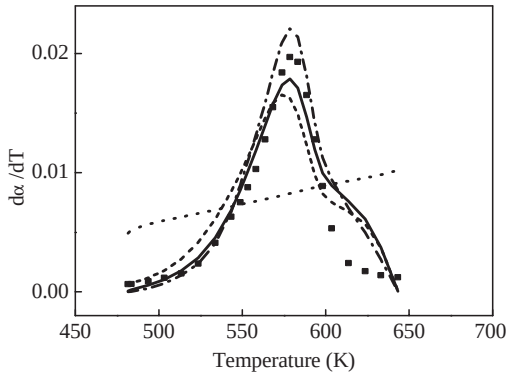

Fig. 10. Simulation of the experimental $(d\alpha/dT)_i$ data with different $f(\alpha)$ models. - - -: model 2, ⋯⋯: model 3, – · –: model 4, ——: model 5, ■: experimental data.

Table 5
The simulation of $f(\alpha)$ with different model functions

No	$f(a)$	M	N	P	A (s^{-1})	E (kJ mol^{-1})	RSS
1	α^m	2.8			2.6×10^{-24}	−240	7.8×10^{-5}
2	$(1-\alpha)^n$		0.88		3.3×10^{6}	93	1.4×10^{-4}
3	$[-\ln(1-\alpha)]^p$			0.022	1.35×10^{-2}	7.6	9.3×10^{-4}
4	$a^m(1-\alpha)^n$	0.92	0.89		1.97×10	32	1.1×10^{-4}
5	$(1-\alpha)^n[-\ln(1-\alpha)]^p$		0.97	0.35	6.5×10^{4}	73.8	8.8×10^{-5}

and growth mechanism. The activation in the thermal-decomposition process is $73.8\,kJ\,mol^{-1}$ and the pre-exponential factor is $1.95 \times 10^4\,s^{-1}$.

4. Conclusion

A novel hydrothermal coating process has been developed to deposit amorphous $Ni(OH)_2 \cdot H_2O$ over octahedral α-Fe_2O_3 particles by treating aqueous dispersion of the preformed cores in $Ni(NO_3)_2$/CH_3COONa solution. The amorphous nickel hydroxide coatings were converted to NiO crystal films after sintering. Increasing sintering temperature or reaction time favored the growth of NiO crystallites. The thermo-decomposition of the $Ni(OH)_2 \cdot H_2O$ coating was a typical process of nucleation and growth, the conversion function of the coating can be expressed as Eq. (10).

Acknowledgments

This project was supported by National Natural Science Foundation of China (No. 50174032).

References

[1] E. Matijevic, Langmuir 1 (1994) 8.
[2] Q.X. Liu, Z.H. Xu, J.A. Finch, R. Egerton, Chem. Mater. 12 (1998) 3936.
[3] V.V. Hardikar, E. Matijevic, J. Colloid Interface 1 (2000) 133.
[4] M. Ohmori, E. Matijevic, J. Colloid Interface Sci. 1 (1993) 288.
[5] D.C. Agrwal, R. Raj, C. Cohen, J. Am. Ceram. Soc. 7 (1990) 2163.
[6] Y. Ohba, T. Watanabe, E. Sakai, M. Daimon, J. Ceram. Soc. Japan 10 (1999) 907.
[7] M.C.D. Andrade, M.R.T. Filgueiras, T. Ogasawara, J. Eur. Ceram. Soc. 4 (2002) 505.
[8] G.J. Li, X.X. Huang, J.K. Guo, Mater. Res. Bull. 7–8 (2001) 1307.
[9] R. Ramaseshan, S.K. Seshadri, N.G. Nair, Scr. Mater. 2 (2001) 183.
[10] B. Pejova, T. Kocareva, M. Najdoski, I. Grozdanov, Appl. Surf. Sci. 165-4 (2000) 271.
[11] I. Haq, K. Akhtar, Adv. Powder Technol. 12 (2000) 175.
[12] C. Li, M.N. Rahaman, J. Am. Ceram. Soc. 7 (1994) 2163.
[13] L. Xiang, K. Sakane, H. Wada, Tsinghua Sci. Technol. 1 (2002) 78.
[14] K.P. Johnston, J.B. Chlistunoff, J. Super-Critical Fluids 12 (1998) 155.
[15] T.M. Mccollom, J.S. Seewald, Geochim. Cosmochim. Acta 19 (2003) 3645.
[16] V. Slovak, Thermochim. Acta 372 (2001) 175.
[17] M. Ping, R.F. Wang, L. Zhao, Thermochim. Acta 296 (1997) 129.
[18] J.J.M. Orfao, F.G. Martins, Thermochim. Acta 390 (2002) 195.
[19] A.W. Coats, J.P. Redfern, Nature 201 (1964) 68.
[20] S. Xing, DTA-TG Analysis and the Non-isothermal Kinetics, Publisher of Metallurgical Industry, Beijing, 1995, 103pp.